Supporting Information

Ionic liquid functionalized injectable and conductive hyaluronic acid hydrogels for the efficient repair of diabetic wounds under electrical stimulation

Pan Liu[a,1], Kai Jin[b,1], Yuange Zong[a], Meng He[a], Chunfeng Lu[a], Huiyue Li[a], Yanying Wang[a], Chunya Li *[,a]

[a]*Key Laboratory of Catalysis and Energy Materials Chemistry of Ministry of Education & Hubei Key Laboratory of Catalysis and Materials Science & Key Laboratory of Analytical Chemistry of the State Ethnic Affairs Commission, South-Central University for Nationalities, Wuhan 430074, China*

[b]*National Engineering Laboratory for Fiber Optic Sensing Technology, Wuhan University of Technology, Wuhan 430074, China*

*Corresponding author. E-mail: lichychem@mail.scuec.edu.cn.

Materials and methods

Characterizations

The ^{1}H-nuclear magnetic resonance (^{1}H-NMR) spectra was collected on an AVANCE 400 NMR system (Bruker, Germany), and DMSO-d_6, D_2O was used as the solvent.

Fourier-transform infrared (FT-IR) spectroscopy analysis was carried out with a Nicolet IS 10 FT-IR spectrometer (Nicolet, USA).

The time-of-flight (TOF) mass spectrum was examined by matrix-assisted laser desorption ionization (MALDI) TOF (Bruker Autoflex Speed, USA) mass spectrometry, and D_2O was used as the solvent.

Scanning electron microscopy (SEM, HITACHI SU8010, Japan) was used to observe the morphologies of the freeze-dried hydrogels.

The mechanical properties of the hydrogels were evaluated with an Instron 5966 universal testing machine. Hydrogels were cut into strips or dumbbells, and testing indicated that their tensile rate was 10 mm/s, and their compressible rate was 2 mm/s.

Solvent replacement method was used to determine the porosity of the hydrogel. Lyophilized hydrogels were weighed (M_0), immersed overnight in absolute ethanol, and blotted with tissue paper to remove excess ethanol from the surface before weighing (M_1). Porosity was calculated using the following equation：Porosity = $(M_1-M_0) / \rho V$. where, M_0 and M_1 represents the masses of hydrogel before and after immersion in absolute ethanol, respectively, ρ represents the density of absolute ethanol, and V represents the volume of the hydrogel.

Rheological properties of the hydrogels

Rheological measurements of the hydrogels were performed by employing a TA rheometer (DHR-2) with parallel-plate geometry (plate diameter of 20 mm, gap of 1000 μm). Next, 250 μL mixed solution of poly ($PBAimBF_4$) and OHA was placed between the parallel plates with a diameter of 20 mm and a gap of 1000 μm. The measurement was performed using a time sweep test with a frequency of 1 Hz and 1% strain.

Cytotoxicity

The cytocompatibility of the PIL-OHA hydrogels was evaluated using the Cell Counting Kit-8 (CCK-8) assay. In a typical assay, the cell suspension was seeded at a density of 5×10^3 cells /100μL per well. After the cells were sufficiently attached to the well, the PIL-OHA hydrogels were disinfected and hydrated, and then placed in the plate. After 72h of culture, the cell proliferation and viability under the hydrogel were evaluated by alamarBlue® assay and the LIVE/DEAD® Viability/Cytotoxicity Kit assay. Then, the optical density (OD) of each well was measured at 450 nm. The relative growth rate (RGR) of cells was used as the index of cytocompatibility.

$$RGR(\%) = \frac{OD_e - OD_{con}}{OD_{neg} - OD_{con}} \times 100$$

where OD_e, OD_{con}, and OD_{neg} denote the optical density of the cells treated with the hydrogels, the medium without cells, and the culture medium, respectively.

Live/dead reagents (Ethidium homodimer-1 (0.5 μM) and calcein AM (0.25 μM)) (Molecular Probes) were added to the samples for 45 min. Then, cell viability was observed by an inverted fluorescence microscope (FV3000, Olympus).

Effects of ES at different frequencies on cell viability

L929 cells (2×10^4 cells /well) were inoculated into a 48-well plate. Sterile and swollen hydrogel was coated onto a cell layer. A custom-made electrode was connected to an alternating power source through a copper wire, and the cells were stimulated with alternating current with a frequency from 25 Hz to 100 Hz and potential from 0 V to 12 V for 1 h every day. CCK-8 analysis was used to evaluate the influence of frequencies on cell survival.

For *in-vitro* scraping tests, a sterile 200-μL pipette tip was used to scrape a cell monolayer in a straight line to simulate an incision wound, which was then washed with PBS to remove cell debris. Four experimental groups were created: (i) Control, (ii) PIL-OHA hydrogel, (iii) Electrode, and (iv) ES+PIL-OHA hydrogel. The cell migration rate was obtained by the following equation:

$$Scratch\ healing\ rate\ \ (\%)\ = \frac{A_{0\ -}\ A_s}{A_0} \times 100$$

where A_0 and A_s denote the scratched area before and after ES, respectively.

Hemolytic activity test of the hydrogels

Rat venous blood was collected using a negative pressure blood collection tube that contained sodium citrate anticoagulant at a ratio of 9:1. Red blood cells were collected by centrifugation at 1000 rpm for 10 min and washed three times with 2 mL PBS until the red color disappeared in the supernatant. In a typical hemolysis assay, 0.8 mL normal saline (negative control group, n = 5), 0.8 mL deionized water (positive control group, n = 5) and 0.8 mL precursor solution (experimental groups, n = 5) were added to the above mentioned diluted red blood cells, which were then incubated in a water bath at 37°C for 3 h. The suspension was centrifuged at 1000 rpm for 10 min. The

absorbance of supernatant was measured at 570 nm using a UV-Vis spectrophotometer. The hemolysis rate of the red blood cells was calculated as follows:

$$Hemolysis\ ratio(\%) = \frac{A_h - A_n}{A_w - A_n} \times 100$$

where A_h, A_n, and A_w denote the absorbance of the sample treated with hydrogel, normal saline, and deionized water, respectively.

Test of the blood clotting ability of the hydrogels

A Kunming mouse (40 g, male) was anesthetized by injecting 10 wt% chloral hydrate, and then, the mouse was fixed on a surgical corkboard. The liver of the mouse was exposed through an abdominal incision, and serous fluid around the liver was carefully removed. A pre-weighed filter paper on a paraffin film was placed beneath the liver. Bleeding from the liver was induced using a 20 G needle with the corkboard tilted at approximately 30°, and 100 μL of PIL-OHA precursor mixture was immediately applied to the bleeding site using the syringe. The filter paper was weighed after 3 min, and the experiment was conducted at least 3 times in parallel.

In *vivo* diabetic wound healing assay

Two weeks after adaptation, mice weighing 35-40 g were randomly selected for injection of streptozotocin (STZ) solution into the abdominal cavity to induce type I diabetes. When the blood glucose concentration continued to exceed 16.7 mmol/L, the diabetic modeling was considered successful. After anaesthetization by 10% chloral hydrate, a square skin defect 8 mm × 8 mm in size was created on the back of the diabetic mouse by removing the entire skin layer down to the muscle membrane. Then, the mice were randomly divided into 7 groups for different treatments. All animal

experiments were approved by the Experimental Animal Ethics Committee of Central South University. The wound healing rate was determined according to the following equation:

$$Wound\ healing\ rate(\%) = \frac{A_0 - A_t}{A_0} \times 100$$

where A_0 denotes the initial area, and A_t denotes the wound area obtained on the 3rd, 7th, and 14th day.

Histology and immunohistochemistry

Diabetic mice were euthanized with an overdose of anesthetics on the 14th day after surgery. Skin tissue samples were removed for histological study. The skin wound tissue was excised, cut into small sections (4 μm), and fixed with 4% formaldehyde in PBS solution. After 24 h, the biopsy tissues were bisected and embedded in paraffin. Finally, the tissue slices were treated with hematoxylin-eosin (H&E) staining for morphological evaluation.

The wound sections were immunohistochemistry stained with tumor necrosis factor (TNF)-α and vascular endothelial growth factor (VEGF) to evaluate inflammation and blood vessel regeneration using a standard protocol. For the immunofluorescence staining of TNF-α, the fixed and frozen regenerated wound tissue sections collected on the 14th day were stained with TNFA antibody at the concentration of 5 μg/mL (Affinity Biosciences). For the immunofluorescence staining of VEGF, the fixed and frozen regenerated wound tissue sections collected on the 14th day were stained with anti-VEGF antibody at the concentration of 5 μg/mL (Abcam). Then, FITC-conjugated goat anti-mouse IgG (cwbiotech) and FITC-conjugated goat anti-rabbit IgG

(cwbiotech) were used as the secondary antibody to reveal TNF-α expression. The nuclei were stained with 4',6-diamidino-2-phenylindole (DAPI) containing mounting solution. Slides was recorded under a fluorescence microscope (TE2000-U; Nikon).

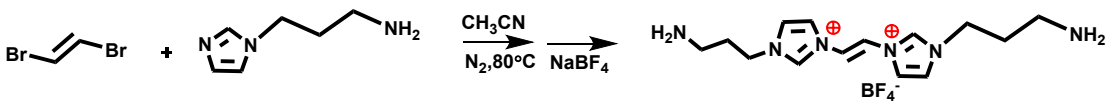

Scheme S1 Schematic graph for the synthesis of $PBAimBF_4$ ionic liquid

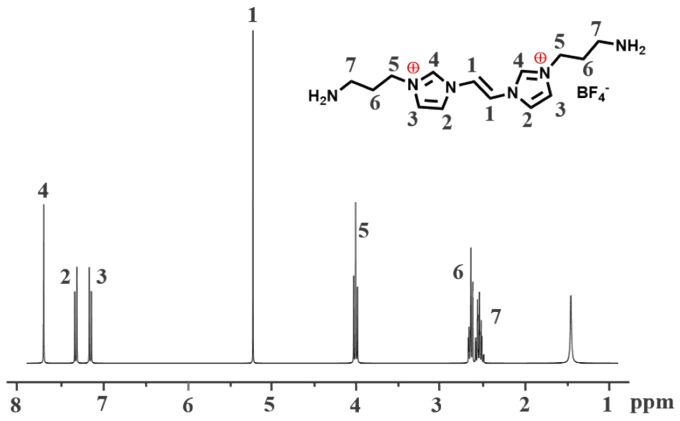

Fig.S1 ^1H NMR spectrum of $PBAimBF_4$ (solvent:D_2O-d_6)

$PBAimBF_4$ was characterized with ^1H-NMR and was shown in **Fig.S1**. ^1H-NMR (δ, D_2O) data are summarized as following: 7.69(s, 2H, H-4), 7.32(d, 2H, H-2), 7.19 (d, 2H, H-3), 5.28 (s, 2H, H-1),4.08 (t, 4H, H-5), 2.72 (m, 4H, H-7), 2.56 (m, 2H, H-6). The result confirmed the successful preparation of the target ionic liquid.

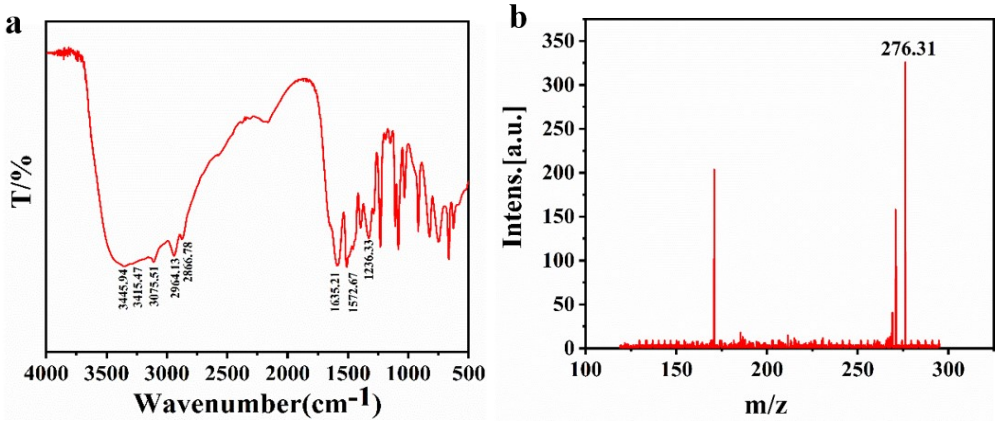

Fig.S2 FT-IR (a) and TOF (b) spectrum of $PBAimBF_4$

FT-IR spectrum of $PBAimBF_4$ was shown in **Fig.S2a**. The absorption peaks located at 3445.94 cm^{-1} and 3415.47 cm^{-1} are the stretching vibration of N-H. 3075.51 cm^{-1} is the stretching vibration of C-H in -CH=CH_2 group.1635.21 cm^{-1},

1572.67 cm^{-1} are ascribed to the skeletal vibration of imidazole ring. The bending vibration peak at 1236.33 cm^{-1} also proved the existence of C=N. The functional groups of $PBAimBF_4$ are presented in FT-IR clearly.

TOF was used to characterize imidazolium cation of $PBAimBF_4$. The result was shown in **Fig.S2b**. The m/z value is 276.31 which is consistent with the formula weight of the PBAim cation of the target compound (276.39), suggesting the successful synthesis of $PBAimBF_4$.

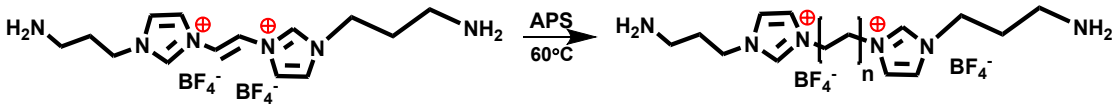

Scheme S2 Schematic graph for the synthesis of poly ($PBAimBF_4$)

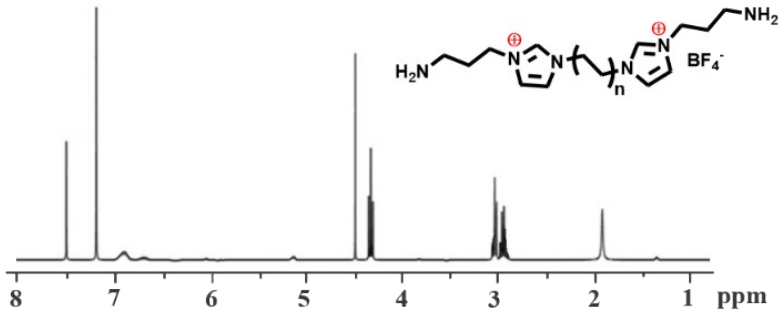

Fig.S3 ^1H NMR spectrum of $PBAimBF_4$ (solvent:D_2O-d_6)

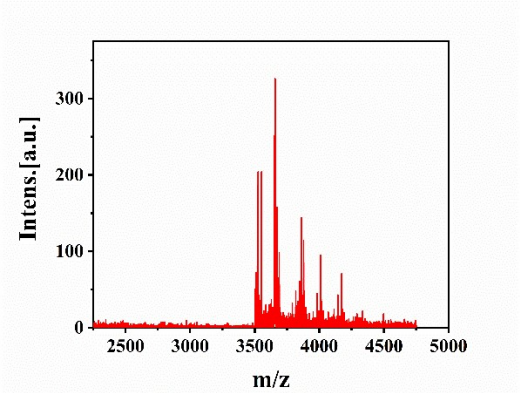

Fig.S4 FT-IR spectrum of $PBAimBF_4$ (solvent:D_2O-d_6)

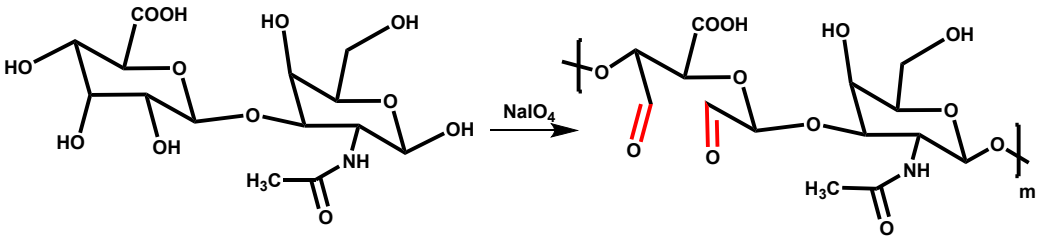

Scheme S3 Schematic graph for the synthesis of OHA

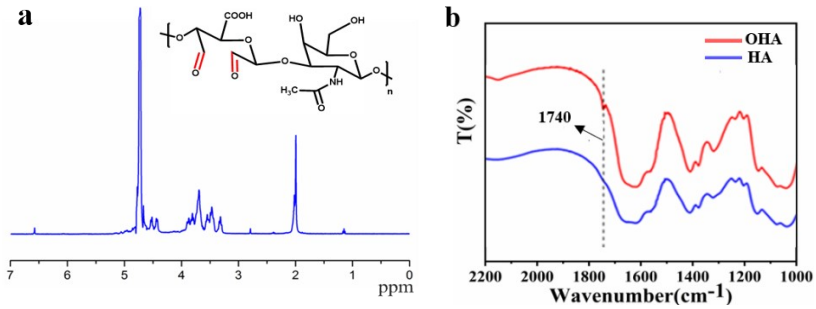

Fig.S5(a) ^{1}H-NMR spectrum of OHA and (b) FTIR spectrum of OHA and HA

OHA was characterized with ^{1}H NMR and was shown in **Fig.S5a**. ^{1}H-NMR (δ, D_2O) data are summarized as following: δ=9.16, 6.57, 4.67, 4.44, 3.81, 3.69, 3.55, 3.47, 3.32, 2.79, 1.99, 1.15. The result confirmed the successful preparation of the OHA.

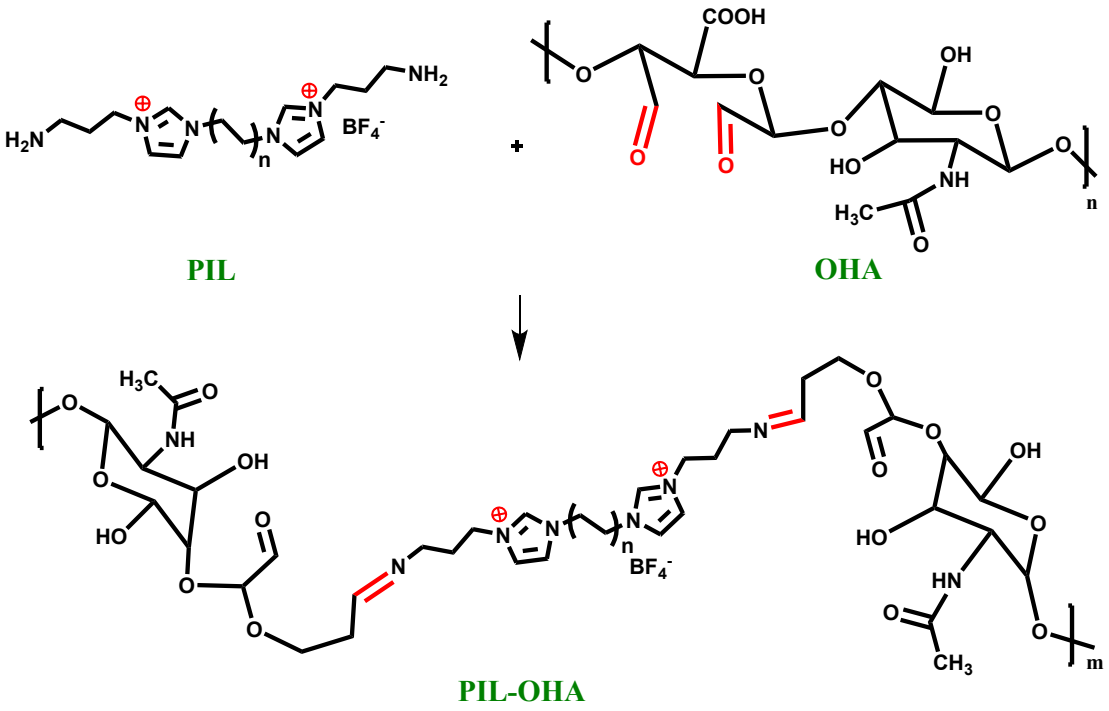

Scheme S4 Chemical cross-linking mechanism of PIL-OHA hydrogels.

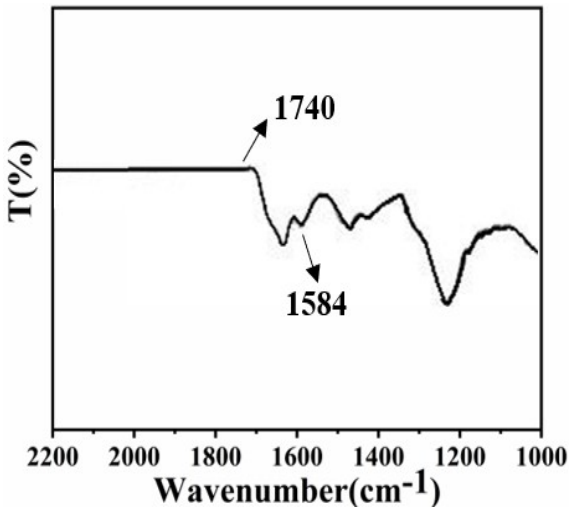

Fig.S6 FT-IR spectrum of PIL-OHA hydrogels

FT-IR was confirmed the successful synthesis PIL-OHA hydrogels. As shown in Fig.S6, the peaks of the N-H functional groups of poly ($PBAimBF_4$) disappeared at 1584 cm^{-1}. Meanwhile, a new stretching vibration peak (1740 cm^{-1}) was formed. This is because after mixing the two solutions, aldehydes reacted with amino groups to form imine bonds.

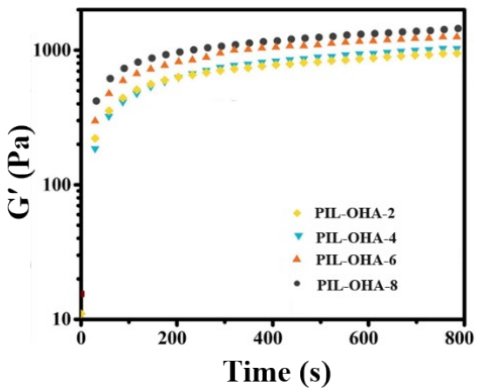

Fig. S7 Rheological behavior of PIL-OHA hydrogels

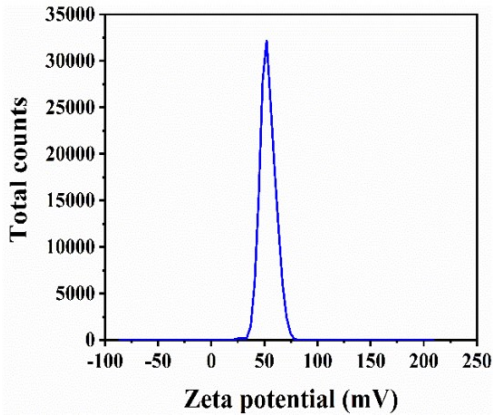

Fig.S8 Zeta potential of PIL-OHA-6